Published in final edited form as:
Magn Reson Imaging. 2013 January ; 31(1): 102–108. doi:10.1016/j.mri.2012.06.018.

Creatine Kinase and ATP Synthase Reaction Rates in Human Frontal Lobe Measured by ^{31}P Magnetization Transfer Spectroscopy at 4T

Fei Du[1,2,*], **Alissa Cooper**[2], **Scott E. Lukas**[1,3], **Bruce M. Cohen**[4], and **Dost Öngür**[2]

[1]Neuroimaging Center, McLean Hospital, Harvard Medical School

[2]Psychotic Disorders Division, McLean Hospital, Harvard Medical School

[3]Behavioral Psychopharmacology Research Laboratory, McLean Hospital, Harvard Medical School

[4]Shervert Frazier Research Institute, McLean Hospital, Harvard Medical School

Abstract

The human frontal lobe is critical for cognitive function in the healthy brain. Many psychiatric disorders including schizophrenia and bipolar disorder are associated with apparent mitochondrial dysfunction and bioenergetic abnormalities in the frontal lobe. Therefore, measuring cerebral bioenergetics associated with creatine kinase (CK) and ATP synthase reactions could provide crucial information regarding the underlying molecular mechanisms associated with psychiatric disorders. In this study, the unidirectional forward chemical exchange metabolic fluxes of creatine kinase and ATP synthase reactions as well as reverse chemical exchange metabolic flux associated with ATP hydrolysis were determined at 4T by ^{31}P magnetization transfer. The current experiments indicate that the kinetic network of $PCr \leftrightarrow ATP \leftrightarrow Pi$ can be measured reliably in the human frontal lobe at 4T, which will enable detailed *in vivo* characterization of bioenergetic abnormalities in a variety of neuropsychiatric disorders.

Keywords

Adenosine triphosphate (ATP); bioenergetics; frontal lobe; ^{31}P MRS; magnetization transfer

INTRODUCTION

Schizophrenia and bipolar disorder are common and severe brain disorders with significant negative impact on the affected individual and on society. Although the exact etiology of these disorders is unknown, numerous *in vivo* studies have demonstrated that abnormalities in neural activity and energy metabolism exist in persons with schizophrenia and bipolar disorder (1–3). Using ^{1}H MRS, our group recently demonstrated that total creatine (tCr) concentrations are reduced in the anterior cingulate cortex and parieto-occipital cortex of patients with schizophrenia (4). *Postmortem* studies also have identified abnormalities in

*Corresponding Author: Fei Du, PhD, McLean Hospital, Department of Psychiatry, Harvard Medical School, 115 Mill St, Belmont MA, 02478, Phone: (617) 855-3945, Fax: (617) 855-3711, fdu@mclean.harvard.edu.

mitochondrial structure (5), dysfunctional oxidative phosphorylation (6), and altered mitochondria related gene expression(7) in schizophrenia and bipolar disorder. Energy production, which largely occurs in mitochondria, is critical for many metabolic and intracellular signaling pathways and for glutamate-glutamine cycling during neurotransmission. Thus, it has great bearing on brain function, including emotional, cognitive and sensorimotor processes. Therefore, quantifying energy metabolism rates *in vivo* may provide crucial information on the pathophysiology of schizophrenia and bipolar disorder and help identify novel targets for drug development.

Adenosine triphosphate (ATP), a high-energy phosphate (HEP) compound, is the universal "energy currency" in living cells (8). It is required to restore cell membrane ion gradients and for most signaling pathways, including intracellular and intercellular signaling. The majority of ATP is formed from adenosine diphosphate (ADP) and inorganic phosphate (Pi) in the mitochondria through oxidative phosphorylation catalyzed by the enzyme ATP synthase (ATP_{syn}) (9). This biochemical process is also coupled to the creatine kinase (CK) reaction linking to phosphocreatine (PCr), which acts as a HEP reservoir and carrier for transferring energy from the mitochondria to the sites of utilization in the cytosol, therefore maintaining a stable ATP level in living cells (10,11). These chemical exchange reactions of $PCr \leftrightarrow ATP \leftrightarrow Pi$ play a fundamental role in cerebral bioenergetics and brain function. Cerebral ATP metabolic rates can be determined explicitly and noninvasively by the *in vivo* ^{31}P magnetization transfer (MT) approach which directly reflects mitochondrial oxidative phosphorylation(12–15).

Although abnormal mitochondrial function in the frontal lobe appears to be associated with psychiatric diseases, CK and ATP_{syn} reaction rates have not previously been measured in this region *in vivo*. In the current study, we explored whether ATP synthesis rates catalyzed by CK and ATP_{syn} can be separately determined in the human frontal lobe at 4T scanner.

METHODS AND MATERIALS

Human subjects and MR imaging

Seventeen healthy human subjects without any psychiatric or substance use disorders (10 males and 7 females, 24.7±4.3 years old) were recruited for these studies. All subjects provided informed consent and the study procedure was approved by the McLean Hospital Institutional Review Board. The MR experiments were conducted using a 4T whole-body scanner interfaced with a Varian INOVA console. Brain anatomic imaging and shimming was conducted by a birdcage volume coil. After global shimming, a 6.5×6.5×5.0 cm^3 voxel within the main sensitivity region of the 7-cm ^{31}P surface coil applied over the frontal lobe was manually shimmed to further minimize magnetic field inhomogeneity (B_0).

In vivo ^{31}P experiments

All the ^{31}P signal was acquired from the sensitivity region of the surface coil except that signal from extra-cranial muscles was eliminated by outer-volume saturation (12). The ^{31}P MT pulse sequence has been described in previous papers, with modification of NMR parameters for the current study. Briefly, a pulse train constructed with multiple hyperbolic Sech pulses with varied RF pulse amplitudes according to the BISTRO scheme (16) was used to saturate selectively the resonance peak of γ-ATP (one-site saturation for measurement of CK and ATP_{syn} reaction rate constants) and both resonances of PCr and Pi (two-site saturation for measurement of the chemical reaction rate constant of ATP hydrolysis to PCr and Pi) (17), in separate experiments. Note that the resonance peak at −2.5 ppm is composed of signal from all nucleoside triphosphates (including ATP, Guanosine-5′-triphosphate and others) and is sometimes referred to as the γ-NTP peak, however, the vast

majority of the signal in this peak arises from ATP and therefore we will refer to it as the γ-ATP peak in this study.

Saturation time was controlled by varying the cycling number of the BISTRO pulse train. For the one-site saturation experiment, a hyperbolic Sech pulse (pulse width = 55 ms, frequency-selective bandwidth = 200 Hz) was applied and saturation time from 0 to 12.73 s was used. For the two-site saturation experiment, the RF pulse described above was modified to saturate PCr and Pi simultaneously. The saturation RF pulse with a single saturation frequency band was replaced by a hyperbolic Sech RF pulse (pulse width = 100 ms) with two identical saturation bands (140-Hz width for each) separated by 360-Hz between the band centers, which equals the chemical shift difference (in Hz) between the PCr and Pi resonance peaks at 4.0 Tesla. Saturation time was varied from 0 to 11.89 s.

The offset RF saturation effect caused by the imperfection of the frequency profile of BISTRO pulse trains was experimentally determined by measuring and comparing the magnetization of chemically non-exchangeable phosphate metabolites acquired in the presence of the BISTRO saturation pulse train at a selected saturation frequency and in the absence of the saturation pulse train. This measurement was performed with varied saturation times. The ratios of these two magnetizations provided the correction factors as a function of the saturation time. The correction factors were applied in the data processing of the saturated *in vivo* ^{31}P spectra in this work.

A 200-μs hard RF pulse was used to excite the phosphate spins and its flip angle (nominal 90°) was adjusted to achieve an optimal NMR signal from the human frontal lobe. *In vivo* ^{31}P spectra were acquired using the following acquisition parameters: 5000 Hz spectral width, 1024 complex data points, 32 and 24 signal averages for the one-site and two-site saturation experiment, respectively. All *in vivo* ^{31}P spectra were acquired with a 14-s repetition time (TR) at the approximately fully relaxed condition. The specific absorption rate (SAR) was maintained below limit of the *US Food and Drug Administration* (FDA).

Due to the relatively long measurement time needed for conducting each *in vivo* ^{31}P MT experiment, 17 subjects were divided into three sub-groups: (i) one-site saturation (n=9), (ii) two-site saturation (n=8, 6 of 8 overlapped with (i)), and (iii) the experiments for determining the offset RF saturation effect (n=6). The total measurement time for each experimental session was ≤ 70 min.

In order to delineate the ^{31}P sensitivity region of the surface coil used in the current experiment setup, 1D profiles of Pi signal along three orthogonal dimensions were acquired from a phantom (14-cm diameter cylindrical bottle) with in-organic phosphate solution ([Pi] = 0.6 M and pH = 7.1).

Spectrum processing

The ^{31}P spectra were analyzed in the time domain using the AMARES algorithm within jMRUI-software package (18). In this study, the initial 4 points of FID (the first 0.9 ms of the signal) were truncated to remove the broad component. Eight resonance peaks (PE: phosphoethanolamine; Pi: inorganic phosphate; GPC: glycerophosphocholine; GPE: glycerophosphoethanolamine; PCr: phosphocreatine; and three adenosine triphosphates: α-, β-, γ-ATP) were included in the basis set. The starting values of spectral resonances positions referred to PCr and line widths were initialed in the spectra fitting. The chemical shift of the PCr resonance peak was assigned to 0 ppm. The spectra base line and zero and first order phase were corrected.

Chemical exchange rates measured by progressive saturation transfer

The chemical exchange reactions among PCr, ATP and Pi were simply illustrated as the Eq. [1], where k_f and k_r are the pseudo first-order forward and reverse rate constant, respectively. For the experiments using progressive saturation on the γ-ATP resonance, the magnetizations of PCr or Pi are governed by the Eqs. [2a] and [2b](19).

$$\mathrm{PCr} \underset{k_r^{\mathrm{ATP}\to\mathrm{PCr}}}{\overset{k_f^{\mathrm{PCr}\to\mathrm{ATP}}}{\rightleftarrows}} \gamma\text{-ATP} \underset{k_r^{\mathrm{ATP}\to\mathrm{Pi}}}{\overset{k_f^{\mathrm{Pi}\to\mathrm{ATP}}}{\leftrightarrows}} \mathrm{Pi} \quad (1)$$

$$\mathrm{M_s(t)}=\mathrm{M_0}\left[\left(\frac{\mathrm{k}}{\alpha}\right)e^{-\alpha t}+\left(\frac{1}{\alpha \mathrm{T_1^{int}}}\right)\right] \quad (2a)$$

$$\alpha=\frac{1}{T_1^{app}}=k+\frac{1}{T_1^{int}} \quad (2b)$$

Where M_s *and* M_0 are the magnetization of PCr, or Pi at saturation time (t) and Boltzmann thermal equilibrium condition, respectively; k is the pseudo first-order forward rate constant involving ATP production via the CK or $\mathrm{ATP_{syn}}$ reaction. T_1^{int} and T_1^{app} are the intrinsic and apparent spin-lattice relaxation times of PCr or Pi, respectively. Therefore k_f of CK and $\mathrm{ATP_{syn}}$ reactions, T_1^{int} and T_1^{app} of PCr and Pi can be determined by fitting the experimental data to a single exponential decay according to Eqs. [2a] and [2b] (14). Similarly, Eqs. [2a] and [2b] also can be used for the two-site (PCr and Pi) saturation experiment (17) except that M refers to magnetizations of γ-ATP. In this case, k is the pseudo first-order reverse rate constant ($k_r^{ATP\to PCr+Pi}$) for ATP utilization via the $\mathrm{ATP_{ase}}$ and reverse CK reactions and

$$k_r^{ATP\to PCr+Pi}=k_r^{ATP\to PCr}+k_r^{ATP\to Pi}$$

T_1^{int} and T_1^{app} are the intrinsic and apparent spin-lattice relaxation time of γ-ATP, respectively.

Lastly, the chemical reaction flux (F) can be calculated by

$$F(\mu mol/g/min)=60\times k\times [M]/1.1 \quad (3)$$

Where, k is forward or reverse chemical exchange constant as described above (s^{-1}) and [M] is the metabolite concentration (μmol/ml) of PCr, Pi and ATP, respectively, according to the one-site or two-site saturation experiment. The chemical reaction fluxes were converted to μmol/g/min assuming brain tissue density of 1.1g/ml.

All data are reported as means +/− one standard deviation.

RESULTS

Phosphate metabolite concentrations and magnetization transfer results

Brain anatomic imaging (in the sagittal orientation) and experiment set-up are illustrated in Fig. 1. The ^{31}P sensitivity region of the surface coil used in the current experiment was

determined as ~160 cc, mainly covering the human frontal lobe. ^{31}P spectra acquired from representative subjects for one-site (γ-ATP) and two-site (PCr and Pi) saturation are shown in Figs. 2 and 3, respectively. The bottom spectra in the Figs. 2 and 3 were acquired in the absence of saturation at approximately full relaxation, and were used to quantify the steady-state concentration of PCr, ATP and Pi. A spectral curve-fitting result is illustrated in Fig. 4, indicating an excellent spectral fitting quality. Based on the measured peak area ratios of PCr, γ-ATP and Pi and [ATP] = 3.0 μmol/ml taken from the literature (20, 21), PCr and Pi concentrations were determined and presented in Table 1. With the progressive increase in saturation time indicated in Fig. 5, magnetizations of PCr and Pi for one-site saturation and γ-ATP for two-site saturation gradually decreased and settled to a low steady-state at the longest saturation times. PCr and Pi magnetization decreased by about 63% and 33% at steady-state while that of γ-ATP decreased by about 37% (see Table 1).

Chemical exchange rate constants and fluxes determined by magnetization transfer experiments

Figs. 5A shows the time dependency of the averaged and normalized resonance peak integrals of PCr and Pi on the saturation time during the progressive saturation experiment and their least-square regression curves according to Eqs. [2a] and [2b]. T_1^{int} and T_1^{app} of PCr and the forward exchange rate constant from PCr to ATP (i.e. $k_f^{PCr\rightarrow ATP}$) were determined as 2.20±0.29 s, 5.80±0.97 s and 0.29±0.04 s^{-1}, respectively. Similarly, T_1^{int} and T_1^{app} of Pi and the forward exchange rate constant from Pi to ATP (i.e., $k_f^{Pi\rightarrow ATP}$) were determined (see Table 1). With the measured concentrations of PCr and Pi, the unidirectional forward chemical exchange fluxes for CK and ATP_{syn} were calculated and all results are listed in Table 1.

Parallel to our γ-ATP saturation experiment, $k_r^{ATP\rightarrow PCr+Pi}$, T_1^{int} and T_1^{app} of γ-ATP were determined by two-site saturation experiments (see Figs. 3 and 5B). Results including the reverse chemical exchange flux are listed in Table 1.

DISCUSSION

We have shown that it is feasible to calculate ATP synthesis and hydrolysis rates for the CK and ATP_{syn}/ATP_{ase} reactions in the human frontal lobe non-invasively at 4T. Our results are broadly consistent with previous work (20, 22–25) as described below, and we extend these findings to include a new brain area that has not been previously studied.

Previous work indicated that *in vivo* ^{31}P MT provides a non-invasive approach for directly studying bioenergetics/mitochondrial function associated with brain activity changes (12–14, 24, 26). The major obstacle to this approach is the low signal-to-noise ratio (SNR) especially for ATP_{syn} reaction measurements because of the intrinsically low nuclear gyromagnetic ratio of ^{31}P and the low concentration of Pi (~1mM). Therefore, to achieve sufficient SNR for ATP_{syn} reaction measurements in this preliminary study, a relatively large region covered by a 7-cm ^{31}P surface coil was studied at 4T, where our group conducts patient-oriented MRS studies based on a private psychiatric hospital. Based on our results of 1D profiles of three orthogonal dimensions, the majority of ^{31}P signal acquired by the 7-cm ^{31}P coil come from the region of the frontal lobe including gray and white matter contributions. In this study we did not conduct an explicit comparison between 4T and our previous data collected at 7T. However, there are some interesting differences between 4T and 7T studies that deserve mention. First, the ^{31}P signal from Pi in the intra-cellular and extra-cellular compartments and GPE/GPC (see Figs. 2 and 3) are resolved at 7T(14) while at 4T they were resolved only 20% of the time (3 subjects out of 17; see Figs. 3 and 4)

despite very good shimming. In the current experiment, the line width of PCr is ~ 14 and 10 Hz without line broadening for the case of Figs. 2 and 3, respectively. Second, T_1^{int} of PCr was 5.80 ± 0.97 s at 4T compared but was much shorter at 7T (4.89 ± 0.54 s) (14). An even shorter T_1^{int} for PCr (3.83±0.57 s) was measured in the rat brain at 9.4T (13). The observed decreases in T_1^{int} of PCr as magnetic field strength increases suggest that the ^{31}P spin of PCr relaxation may be dominated by the chemical shift anisotropy (CSA) mechanism (27). By contrast, T_1^{int} of Pi was calculated at 3.56 ± 0.72 s, 3.77 ± 0.53 s and 4.03 ± 0.64 s at 4T, 7T and 9.4T, respectively (13,14), with the significant difference between 4T and 7T on the one hand and 9.4T on the other (p=0.007, two-tailed t-test). This relationship demonstrates that the intrinsic T_1 of Pi increases with the magnetic field strength and the ^{31}P spin of Pi relaxation may be dominated by dipolar interactions (27). T_1^{int} of γ-ATP was calculated as 1.42 ± 0.21 s in the current 4T study, which is similar to observations at 7T and 9.4T (~1.35 s and ~1.24 s in human and rat brain, respectively) (13,14,28). Again, this observation indicates that the field dependence of phosphate T_1 is mainly due to two competing relaxation mechanisms, CSA and dipolar interactions. The intrinsic relaxation times of PCr, γ-ATP and Pi were compared in the current study, but similar trends have been observed in previous studies measuring T_1 via a conventional inversion recovery method and single exponential curve fitting (29,30). T_1 measurements for PCr, γ-ATP and Pi would be affected by the chemical exchange rate constants since the three metabolites are involved in chemical reactions with one another (31).

In addition to measuring the unidirectional forward chemical exchange fluxes of CK and ATP_{syn} reactions and simultaneously the intrinsic relaxation times of PCr and Pi in one set of experiments, we measured the reverse chemical exchange flux and the γ-ATP intrinsic relaxation time by saturating PCr and Pi simultaneously in another. The apparent total ATP hydrolysis rate constant, $k_r^{ATP\rightarrow PCr+Pi}$, were determined as 0.43 ± 0.07 s^{-1}. Using the unidirectional forward chemical exchange constants calculated from saturating γ-ATP and concentrations of PCr, ATP and Pi, as well as a chemical balance condition assumption, the reverse chemical exchange rate constant of ATP hydrolysis to PCr and Pi were deduced as 0.45 ± 0.06 s^{-1}, very similar to the value (0.43 ± 0.07 s^{-1}) directly determined by the two-site saturation experiment and not significant difference. Therefore, the current experiments measuring forward and reverse chemical reaction fluxes indicate that the chemical reactions among PCr, ATP and Pi are at an approximately balanced condition and the simple global chemical exchange model of PCr↔ATP↔Pi can be used to measure energy production and utilization in a combined ^{31}P magnetization transfer strategy.

One methodological limitation of conventional ^{31}P magnetization transfer approaches is the relatively long acquisition time (14, 19, 32–40), which prevents adequate temporal resolution for dynamic studies such as monitoring acute drug effects. For instance, the current measurements were performed with a 14-s repetition time at an approximately (although perhaps not completely) fully relaxed condition.

Some novel ^{31}P MT approaches such as FAST and TRIST aim to measure the same chemical reaction fluxes (41, 42). Recently, we developed a ^{31}P MT MRS approach (T_1^{nom}), aimed at rapidly mapping energy-ATP metabolic fluxes (28,43). Using this approach, only 2 spectra with optimized flip angles (β) and TR need be obtained to calculate chemical exchange fluxes of the CK and ATP_{syn} reactions as long as the intrinsic relaxation times of PCr, γ-ATP and Pi are known. The great advantage of this approach is that the acquisition time is significantly shorter, enabling improved SNR, increased spatial/temporal resolution, and higher reliability. Our current measurements lay the groundwork for rapid

acquisition ^{31}P MT MRS with the increased spatial and temporal resolution by establishing the necessary T_1^{int} values for the relevant metabolites in the healthy human frontal lobe at 4T.

In summary, a ^{31}P MT approach to measure ATP metabolic rates in the human frontal lobe was applied in the current study. Specifically, the unidirectional forward chemical exchange metabolic fluxes of the CK and ATP_{syn} reactions and reverse chemical exchange metabolic flux associated with ATP hydrolysis were determined at 4T. Thus, the current experiments indicate the kinetic network of $PCr \leftrightarrow ATP \leftrightarrow Pi$ can be measured in human frontal lobe at 4T by using *in vivo* ^{31}P MT. This work provides a foundation for future studies of bioenergetics/mitochondrial function in a variety of neuropsychiatric disorders at our 4T scanner.

Acknowledgments

This work was partially supported by NIH grants: 1R21MH092704, 5K23MH079982 and 5T32DA015036.

References

1. Rezin GT, Amboni G, Zugno AI, Quevedo J, Streck EL. Mitochondrial dysfunction and psychiatric disorders. Neurochem Res. 2009; 34(6):1021–1029. [PubMed: 18979198]
2. Stork C, Renshaw PF. Mitochondrial dysfunction in bipolar disorder: evidence from magnetic resonance spectroscopy research. Mol Psychiatry. 2005; 10 (10):900–919. [PubMed: 16027739]
3. Smesny S, Rosburg T, Nenadic I, Fenk KP, Kunstmann S, Rzanny R, Volz HP, Sauer H. Metabolic mapping using 2D ^{31}P-MR spectroscopy reveals frontal and thalamic metabolic abnormalities in schizophrenia. Neuroimage. 2007; 35(2):729–737. [PubMed: 17276699]
4. Ongur D, Prescot AP, Jensen JE, Cohen BM, Renshaw PF. Creatine abnormalities in schizophrenia and bipolar disorder. Psychiatry Res. 2009; 172(1):44–48. [PubMed: 19239984]
5. Cataldo AM, McPhie DL, Lange NT, Punzell S, Elmiligy S, Ye NZ, Froimowitz MP, Hassinger LC, Menesale EB, Sargent LW, Logan DJ, Carpenter AE, Cohen BM. Abnormalities in mitochondrial structure in cells from patients with bipolar disorder. Am J Pathol. 177(2):575–585. [PubMed: 20566748]
6. Marchbanks RM, Mulcrone J, Whatley SA. Aspects of oxidative metabolism in schizophrenia. Br J Psychiatry. 1995; 167(3):293–298. [PubMed: 7496636]
7. Ben-Shachar D, Laifenfeld D. Mitochondria, synaptic plasticity, and schizophrenia. Int Rev Neurobiol. 2004; 59:273–296. [PubMed: 15006492]
8. Attwell D, Laughlin SB. An energy budget for signaling in the grey matter of the brain. Journal of Cerebral Blood Flow & Metabolism. 2001; 21(10):1133–1145. [PubMed: 11598490]
9. Slater EC, Holton FA. Oxidative phosphorylation coupled with the oxidation of alpha-ketoglutarate by heart-muscle sarcosomes. I. Kinetics of the oxidative phosphorylation reaction and adenine nucleotide specificity. Biochem J. 1953; 55(3):530–544. [PubMed: 13105665]
10. Saks VA, Ventura-Clapier R, Aliev MK. Metabolic control and metabolic capacity: two aspects of creatine kinase functioning in the cells. Biochim Biophys Acta. 1996; 1274(3):81–88. [PubMed: 8664307]
11. Kemp GJ. Non-invasive methods for studying brain energy metabolism: what they show and what it means. Dev Neurosci. 2000; 22(5–6):418–428. [PubMed: 11111158]
12. Chaumeil MM, Valette J, Guillermier M, Brouillet E, Boumezbeur F, Herard AS, Bloch G, Hantraye P, Lebon V. Multimodal neuroimaging provides a highly consistent picture of energy metabolism, validating ^{31}P MRS for measuring brain ATP synthesis. Proc Natl Acad Sci U S A. 2009; 106(10):3988–3993. [PubMed: 19234118]
13. Du F, Zhu XH, Zhang Y, Friedman M, Zhang N, Ugurbil K, Chen W. Tightly coupled brain activity and cerebral ATP metabolic rate. Proc Natl Acad Sci U S A. 2008; 105(17):6409–6414. [PubMed: 18443293]

14. Du F, Zhu XH, Qiao H, Zhang X, Chen W. Efficient in vivo ^{31}P magnetization transfer approach for noninvasively determining multiple kinetic parameters and metabolic fluxes of ATP metabolism in the human brain. Magn Reson Med. 2007; 57(1):103–114. [PubMed: 17191226]
15. Brown TR, Ugurbil K, Shulman RG. ^{31}P nuclear magnetic resonance measurements of ATPase kinetics in aerobic Escherichia coli cells. Proc Natl Acad Sci U S A. 1977; 74(12):5551–5553. [PubMed: 146199]
16. de Graaf RA, Luo Y, Garwood M, Nicolay K. B1-insensitive, single-shot localization and water suppression. J Magn Reson B. 1996; 113(1):35–45. [PubMed: 8888589]
17. Spencer RG, Balschi JA, Leigh JS Jr, Ingwall JS. ATP synthesis and degradation rates in the perfused rat heart ^{31}P-nuclear magnetic resonance double saturation transfer measurements. Biophys J. 1988; 54(5):921–929. [PubMed: 3242635]
18. van den Boogaart, A.; Van Hecke, A.; Van Huffel, P.; Graveron-Demilly, S.; van Ormondt, D.; de Beer, R. MRUI: a graphical user interface for accurate routine MRS data analysis. Prague; 1996. p. 318
19. Degani H, Laughlin M, Campbell S, Shulman RG. Kinetics of creatine kinase in heart: a ^{31}P NMR saturation- and inversion-transfer study. Biochemistry. 1985; 24(20):5510–5516. [PubMed: 4074712]
20. Hetherington HP, Spencer DD, Vaughan JT, Pan JW. Quantitative ^{31}P spectroscopic imaging of human brain at 4 Tesla: assessment of gray and white matter differences of phosphocreatine and ATP. Magn Reson Med. 2001; 45(1):46–52. [PubMed: 11146485]
21. Siesjo, BK. Brain energy metabolism. New York: Wiley; 1978. p. 101-110.
22. Mora BN, Narasimhan PT, Ross BD. ^{31}P magnetization transfer studies in the monkey brain. Magn Reson Med. 1992; 26(1):100–115. [PubMed: 1625557]
23. Mlynarikv, ZS.; Brehm, A.; Bischof, M.; Roden, M. An optimized protocol for measuring rate constant of creatine kinase reaction in human brain by ^{31}P NMR saturation transfer. 13th Proc Intl Soc Mag Reson Med; 2005. p. 2767
24. Lei H, Ugurbil K, Chen W. Measurement of unidirectional Pi to ATP flux in human visual cortex at 7 T by using in vivo ^{31}P magnetic resonance spectroscopy. Proc Natl Acad Sci U S A. 2003; 100(24):14409–14414. [PubMed: 14612566]
25. Mason GF, Chu WJ, Vaughan JT, Ponder SL, Twieg DB, Adams D, Hetherington HP. Evaluation of ^{31}P metabolite differences in human cerebral gray and white matter. Magn Reson Med. 1998; 39(3):346–353. [PubMed: 9498589]
26. Du F, Zhang Y, Iltis I, Marjanska M, Zhu XH, Henry PG, Chen W. In vivo proton MRS to quantify anesthetic effects of pentobarbital on cerebral metabolism and brain activity in rat. Magn Reson Med. 2009; 62(6):1385–1393. [PubMed: 19780161]
27. Evelhoch JL, Ewy CS, Siegfried BA, Ackerman JJ, Rice DW, Briggs RW. ^{31}P spin-lattice relaxation times and resonance linewidths of rat tissue in vivo: dependence upon the static magnetic field strength. Magn Reson Med. 1985; 2(4):410–417. [PubMed: 4094555]
28. Xiong Q, Du F, Zhu X, Zhang P, Suntharalingam P, Ippolito J, Kamdar FD, Chen W, Zhang J. ATP production rate via creatine kinase or ATP synthase in vivo: a novel superfast magnetization saturation transfer method. Circ Res. 108(6):653–663. [PubMed: 21293002]
29. Qiao H, Zhang X, Zhu XH, Du F, Chen W. In vivo ^{31}P MRS of human brain at high/ultrahigh fields: a quantitative comparison of NMR detection sensitivity and spectral resolution between 4 T and 7 T. Magn Reson Imaging. 2006; 24(10):1281–1286. [PubMed: 17145398]
30. Bogner W, Chmelik M, Schmid AI, Moser E, Trattnig S, Gruber S. Assessment of ^{31}P relaxation times in the human calf muscle: a comparison between 3 T and 7 T in vivo. Magn Reson Med. 2009; 62(3):574–582. [PubMed: 19526487]
31. Horska A, Horsky J, Spencer RGS. Measurement of Spin-lattice Relaxation Times in Systems Undergoing Chemcial Exchange. J Magn Reson Series A. 1994; 110:82–89.
32. Weiss RG, Gerstenblith G, Bottomley PA. ATP flux through creatine kinase in the normal, stressed, and failing human heart. Proc Natl Acad Sci U S A. 2005; 102(3):808–813. [PubMed: 15647364]

33. Joubert F, Mateo P, Gillet B, Beloeil JC, Mazet JL, Hoerter JA. CK flux or direct ATP transfer: versatility of energy transfer pathways evidenced by NMR in the perfused heart. Mol Cell Biochem. 2004; 256–257(1–2):43–58.
34. Mora BN, Narasimhan PT, Ross BD. ^{31}P magnetization transfer studies in the monkey brain. Magnetic Resonance in Medicine. 1992; 26(1):100–115. [PubMed: 1625557]
35. Bottomley PA, Hardy CJ. Maping creatine kinase reaction rates in human brain and heart with 4 Tesla saturation transfer ^{31}P NMR. Journal of Magnetic Resonance. 1992; 99:443–448.
36. Mora B, Narasimhan PT, Ross BD, Allman J, Barker PB. ^{31}P saturation transfer and phosphocreatine imaging in the monkey brain. Proc Natl Acad Sci U S A. 1991; 88(19):8372–8376. [PubMed: 1924297]
37. Brindle KM, Blackledge MJ, Challiss RA, Radda GK. ^{31}P NMR magnetization-transfer measurements of ATP turnover during steady-state isometric muscle contraction in the rat hind limb in vivo. Biochemistry. 1989; 28(11):4887–4893. [PubMed: 2765517]
38. Bottomley PA, Hardy CJ, Roemer PB, Weiss RG. Problems and expediencies in human ^{31}P spectroscopy. The definition of localized volumes, dealing with saturation and the technique-dependence of quantification. NMR in Biomedicine. 1989; 2(5–6):284–289. [PubMed: 2641902]
39. Spencer RG, Balschi JA, Leigh JS Jr, Ingwall JS. ATP synthesis and degradation rates in the perfused rat heart ^{31}P-nuclear magnetic resonance double saturation transfer measurements. Biophysical Journal. 1988; 54(5):921–929. [PubMed: 3242635]
40. Sture Forsen RAH. Study of moderately rapid chemical exchange reactions by means of nuclear magnetic resonance. The Journal of Chemical Physics. 1963; 39(11):2892–2901.
41. Bottomley PA, Ouwerkerk R, Lee RF, Weiss RG. Four-angle saturation transfer (FAST) method for measuring creatine kinase reaction rates in vivo. Magn Reson Med. 2002; 47(5):850–863. [PubMed: 11979563]
42. Schar M, El-Sharkawy AM, Weiss RG, Bottomley PA. Triple repetition time saturation transfer (TRiST) ^{31}P spectroscopy for measuring human creatine kinase reaction kinetics. Magn Reson Med. 63(6):1493–1501. [PubMed: 20512852]
43. Du, F.; Xiong, Q.; Zhu, X-H.; Chen, W. An Improved Magnetization Saturation Transfer Approach---T_1^{nom} for Rapidly Measuring and Quantifying CK Activity in the Rat Brain. Stockholm, Sweden: 2010. p. 1111

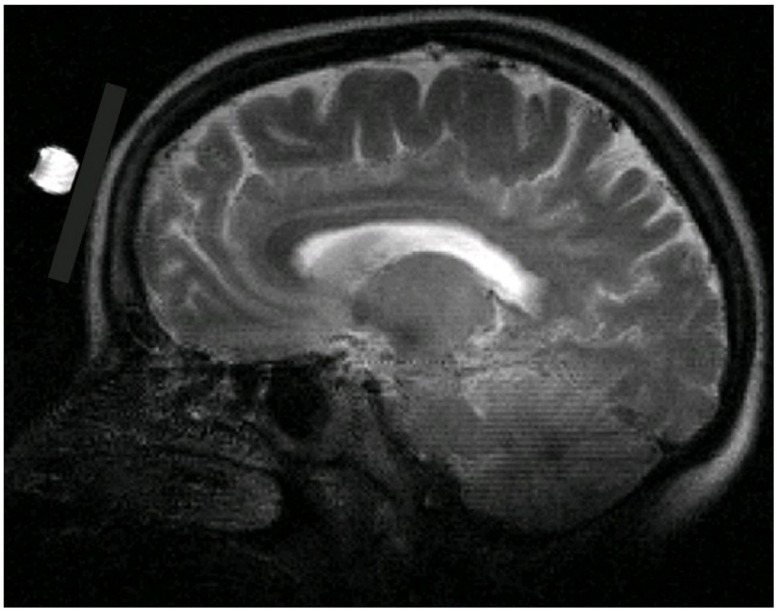

Fig. 1.
T_2-weighted Brain anatomic imaging (in the sagittal orientation) with a 7-cm ^{31}P surface coil. ^{31}P surface coil position is illustrated by a 1-cm sphere with the saline solution at the center of ^{31}P surface coil.

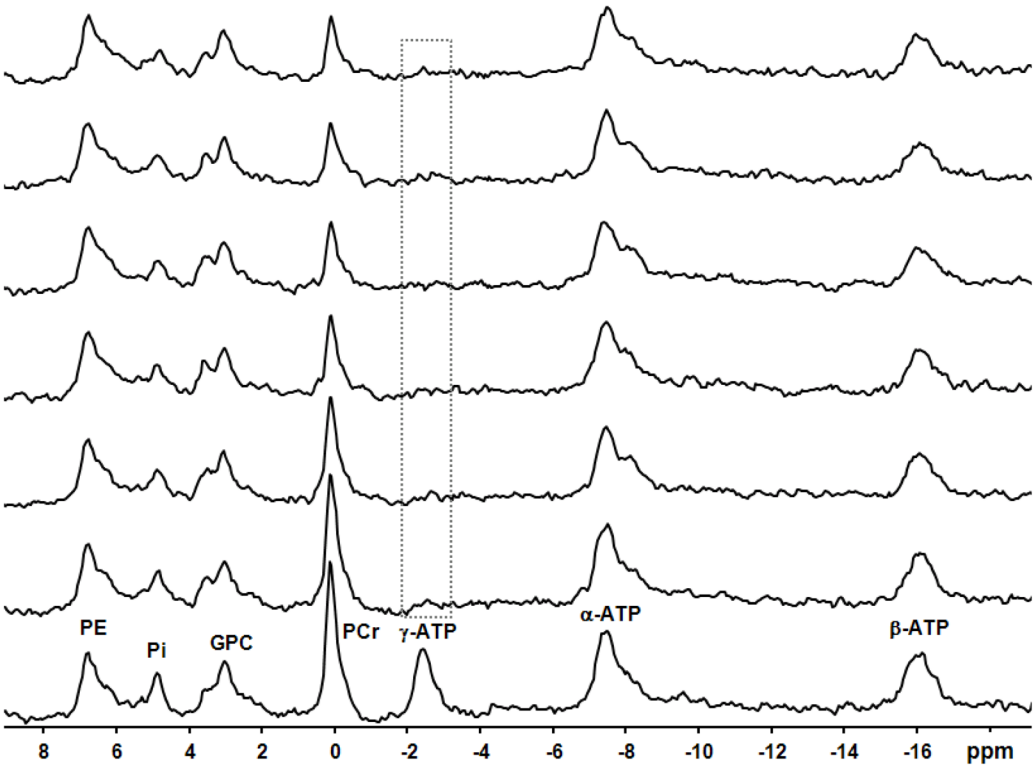

Fig. 2.

In vivo ^{31}P spectra with 10-Hz line broadening of a representative subject in the absence and presence of complete saturation (lowest spectrum and all higher ones, respectively) on the γ-ATP resonance (illustrated by the box) with varied saturation times (from 0 to 12.73 s, longer saturation times presented in progressively higher spectra). All resonance peaks are labeled in the lowest spectrum.

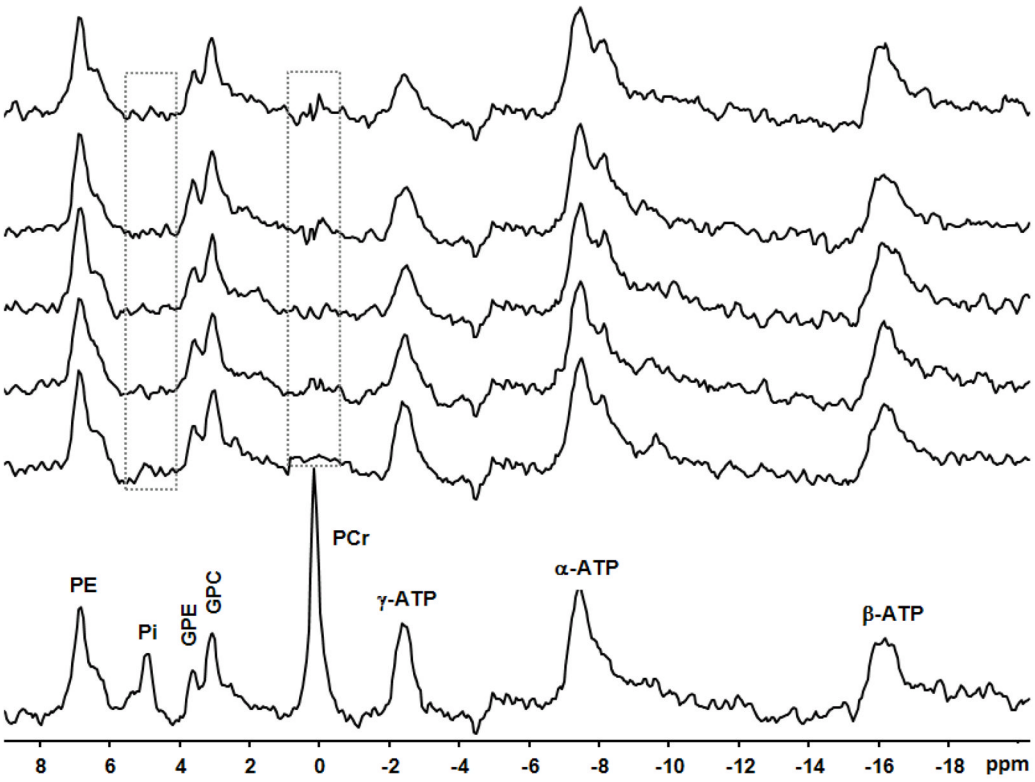

Fig. 3.

In vivo ^{31}P spectra with 10-Hz line broadening of a representative subject in the absence and presence of complete saturation (lowest spectrum and all higher ones, respectively) on the PCr and Pi resonances (illustrated by the boxes) with varied saturation times (0 to 11.89 s, longer saturation times presented in progressively higher spectra).

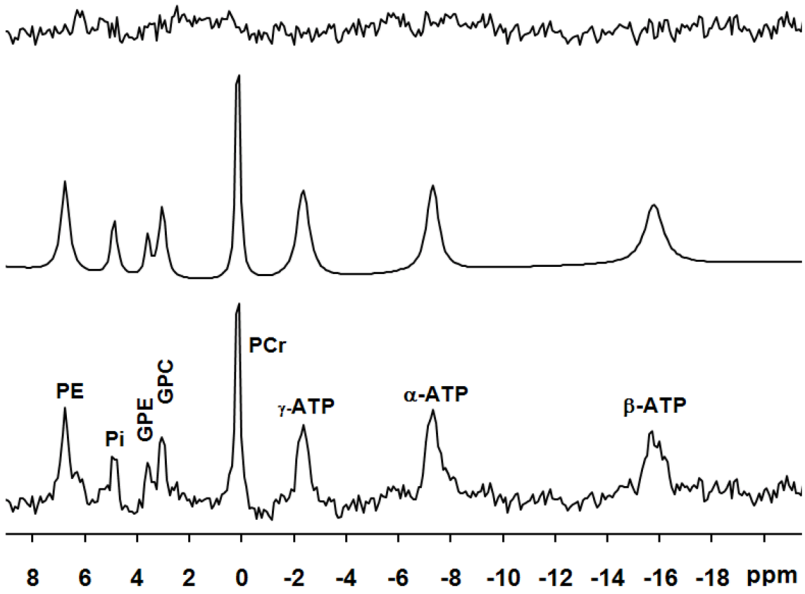

Fig. 4.

A ^{31}P spectrum (bottom) acquired from the frontal lobe of a representative subject and its fitted spectrum (middle) and residue (upper). A line-broadening of 6 Hz was applied to display the spectra.

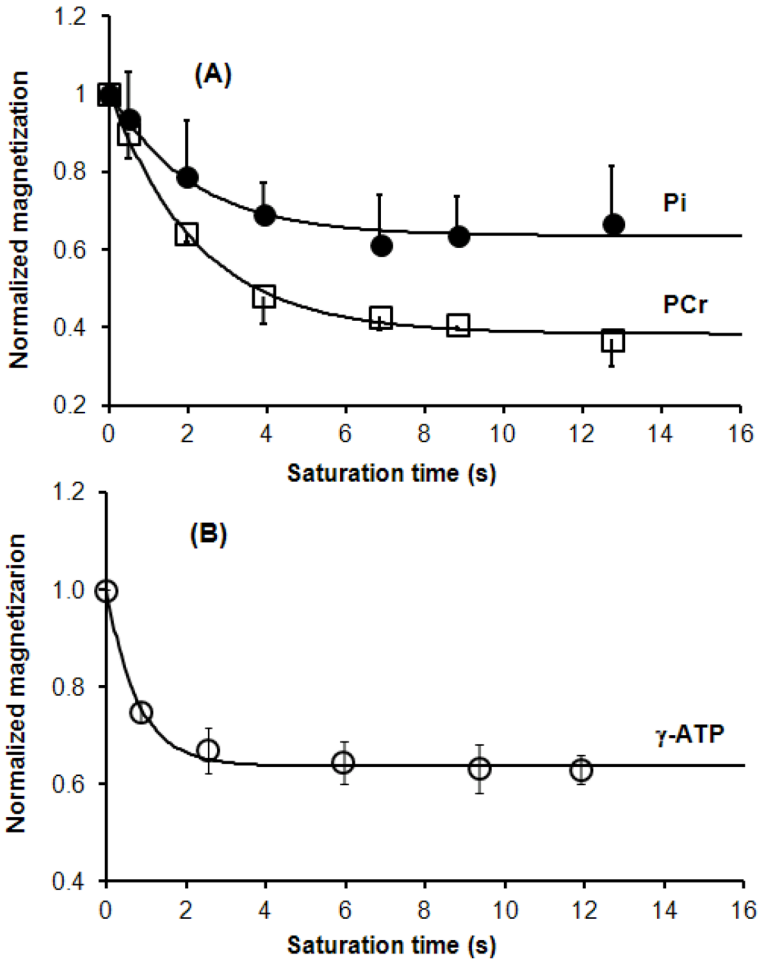

Fig. 5.

Dependence of the averaged normalized resonance peaks integrals on the saturation time for one-site saturation (A, n=9) and two-site saturation (B, n=8), respectively. The peak integrals represent the normalized M_s/M_0 ratios with the correction of offset RF saturation effect. The apparent and intrinsic spin-lattice relaxation times of PCr and Pi, the forward rate constants ($k_f^{PCr\rightarrow ATP}$ and $k_f^{Pi\rightarrow ATP}$), were determined by the regression analyses presented in (A). The apparent and intrinsic spin-lattice relaxation times of γ-ATP, the reverse rate constant ($k_r^{ATP\rightarrow PCr+Pi}$), were determined by the least-square regression and presented in (B).

Table 1

Results of Magnetization Saturation Transfer Measurements in the Human Frontal lobe

	Sat (γ-ATP)	Sat (PCr and Pi)
Subject #	**N=9**	**N=8**
Concentration (μmol/ml)	[PCr]=4.13±0.40; [Pi]=1.09±0.17	[PCr]=4.14±0.62; [Pi]=1.08±0.21
M*/M₀ of PCr	0.37±0.07	—
***M*/M₀ of γ*-ATP	—	0.63± 0.05
M*/M₀ of Pi	0.67±0.11	—
Rate constant (s^{-1})	$k_f^{PCr\rightarrow ATP}=0.29\pm0.04$ $k_f^{Pi\rightarrow ATP}=0.16\pm0.06$	$k_r^{ATP\rightarrow PCr+Pi}=0.43\pm0.07$
T₁ (s)	$T_1^{app}(PCr)=2.20\pm0.29$ $T_1^{int}(PCr)=5.80\pm0.97$ $T_1^{app}(Pi)=2.30\pm0.58$ $T_1^{int}(Pi)=3.56\pm0.72$	$T_1^{app}(\gamma-ATP)=0.82\pm0.14$ $T_1^{int}(\gamma-ATP)=1.42\pm0.21$
Chemical exchange flux (μmol/g/min)	$F_f^{PCr\rightarrow ATP}=65.55\pm12.11$ $F_f^{Pi\rightarrow ATP}=8.88\pm3.68$	$F_r^{ATP\rightarrow PCr+Pi}=70.36\pm11.45$